Columbia International Publishing
Journal of Advanced Electrical and Computer Engineering
(2014) Vol. 1 No. 1 pp. 22-31

Research Article

Effect of Pulse Shaping on Autocorrelation Function of Barker and Frank Phase Codes

Praveen Ranganath[1*] and Sathyanarayan Rao[1]

Received 12 May 2014; Published online 28 June 2014

Abstract

Phase coded pulse-compression is a commonly used technique in a variety of applications; for example to improve resolution in range-finding applications. In this paper, we consider two phase codes- binary Barker code of length 13 and polyphase Frank code of length 9. The effects of using four different pulse shapes (Rectangular, Triangular, Gaussian, and Exponential) on these two phase codes are assessed using the autocorrelation function. The performance parameters (Peak Sidelobe Level (*PSL*), Integrated Sidelobe Level (*ISL*), and 3dB mainlobe widths) derived from the autocorrelation function are compared and discussed. Possible applications are discussed based on the excellent properties demonstrated by exponential pulse shape for these two phase codes.

Keywords: Phase codes, Pulse shape, Autocorrelation, 3dB width, Peak and Integrated sidelobe levels

1. Introduction

Pulse compression is a phase-coded modulation technique employed to improve the range resolution in radar signals. In this technique, each chip within a pulse is modulated in accordance to the sequence of phases defined by the code. The codes are either real binary or complex poly phase-codes. One such set of commonly used binary codes in phase modulation is the well known classical Barker codes (Barker, 1953). Barker codes have been under study since 1950s, due to their low autocorrelation binary sequences. Similar to binary codes, polyphase codes are also used. One such popular polyphase code is the Frank code (Frank, 1963).

Pulse shaping is an important aspect to be considered while designing wireless systems such as radar and communication systems. Pulse shaping enhances the performance of a communication system by reducing intersymbol interference and dispersion (Schafhuber et al., 2002). The

*Corresponding e-mail: pr0007@alumni.uah.edu
1 Member, Alumni Association, The University of Alabama in Huntsville, USA

characteristics of a modulated pulse, or a waveform in general, can be described by its autocorrelation function. Some of the common derived quantities of autocorrelation function used in describing the performance of a waveform are the peak sidelobe level (***PSL***), integrated sidelobe level (***ISL***), energy, and 3dB resolution widths. For example, in the case of range-finding systems, the ***PSL*** is related to rejecting unwanted returning signals from point sources around the region of interest where the range-finding is performed. The ***ISL*** is associated with the suppressing the distributed returns near the area of interest (Nunn & Coxson, 2008). Due to excellent bandwidth offered by optical fibers, pulse shaping of laser beams has become an important research area in the recent years (Li, 2009; Wiener, 2011). It is also an important parameter to be considered in radar signal processing, for example, pulse shape of the transmitted signal determines the range resolution, minimum and maximum range of a range-finding device. One recent study by Yurchak (2012) describes the pulse shaping effect on echo waveform of radar altimeter.

In this work we have investigated the effect of four different pulse shapes on autocorrelation properties of the classical Barker code and Frank code. The set of pulse shapes implemented in this paper consists of Rectangular, Triangular, Gaussian and Exponential pulses on the Barker-13, and Frank-9 phase codes. Barker-13 code is a binary code with 13 chips, while Frank-9 code is a complex polyphase code with 9 chips. While confining the discussion only to two phase codes and four pulse shapes, this paper illustrates the basic idea of effect of pulse shaping on autocorrelation parameters such as ***ISL***, ***PSL*** and 3dB widths. This study could be of great relevance to the areas where pulse shaping and phase codes are routinely used.

The remaining sections of this paper are organized as follows. In section 2, the mathematical notations of the performance parameters are discussed. In Section 3, the above mentioned pulse shapes and the two phase codes are implemented and the autocorrelation functions are computed. The qualities of each phase-code modulated pulse are derived and described in Section 4. Finally, based on the observations, we conclude our work in Section 5 with a discussion on the exponential pulse.

2. Performance Parameters

2.1 Autocorrelation

When two signals under comparison are identical, then the cross correlation operation is called autocorrelation. Mathematically, the autocorrelation function of a discrete finite sequence $x[n], (n = 1, 2, \ldots, N)$ is given by the following equation

$$R_x(t) = \sum_{i=1}^{N-t} x[i]x^*[i+t] \tag{1}$$

where $t = 0, 1, \ldots, N-1$ is the discrete time-index, the asterisk on the second term in the product of the right side of Eq. 1 denotes the complex conjugate. The negative half sequence of the autocorrelation function is the mirrored complex conjugate of the corresponding positive sequence sequence given by

$$R_x(-t) = R_x^*(t) \tag{2}$$

The signal $x[n]$ could be a real signal as in classical Barker code, or a complex signal such as in the Frank code. Since autocorrelation function measures similarity of a signal with itself, there will be a maximum peak value when the two sequences under consideration are aligned. In other words, the function $R_x(t)$ will have a peak at $t=0$. In locations other than $t=0$, the magnitude of the autocorrelation $R_x(t)$ will have lower values. Usually in radar signal processing, the received pulse is correlated with a copy of transmitted pulse and the resulting function gives information about the range of the target. In strict sense, since received signal is different from the transmitted pulse, it is cross correlation operation. But however, using the autocorrelation function, we can describe three commonly used performance parameters and it applies to scenario where cross correlation is performed such as radar signal processing.

2.2 Peak Sidelobe Level

For illustration purposes, we have considered a simple rectangular pulse shape and Fig. 1 shows its autocorrelation function which is computed using Eq. 1. In this figure, the central dark peak between time lag $R_x(0)$ and $\pm\tau_c$ is called the mainlobe and the lighter shaded peaks between time lag $\pm(\tau_c+1)$ to $\pm N_c\tau_c$ are referred as sidelobes. The absolute maximum value among the secondary peaks in the sidelobes is the peak sidelobe level (*PSL*) or the first sidelobe level (Richards et. al., 2010), which is expressed as

$$PSL = \max_{t \neq 0}\{R_x(t)\}. \tag{3}$$

This quantity is more often expressed as a ratio relative to the mainlobe level in decibels, defined as the peak sidelobe level ratio (*PSLR*). The *PSLR* in decibels is represented as

$$PSLR[dB] = 20\log_{10}\left(\frac{PSL}{R_x(0)}\right). \tag{4}$$

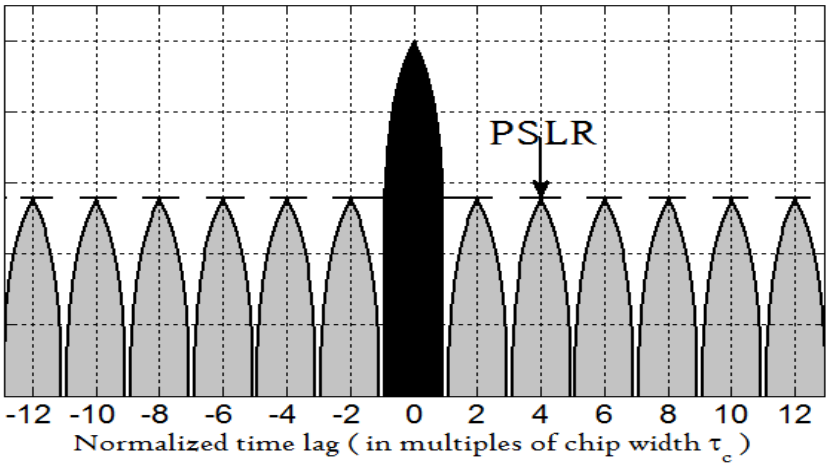

Fig. 1. Illustrating the autocorrelation parameters

2.3 Energy

The sequences in the autocorrelation function contribute individually to the total energy content of the signal. The energy of a finite sequence $x[n], (n = 1, 2, \ldots, N)$, using the expression for the autocorrelation function, is computed as

$$E = 2\sum_{t=1}^{N-1} R_x^2(t). \tag{5}$$

2.4 Integrated Sidelobe Level

Apart from the ***PSL*** in describing the performance of the sidelobes, another important performance parameter of the autocorrelation function is the Integrated Sidelobe-level (***ISL***). The Integrated sidelobe level is defined (Richards et. al., 2010) as

$$ISL = \frac{Energy\ in\ Sidelobes\ (\text{lighter region})}{Energy\ in\ Mainlobe\ (\text{dark region})}. \tag{6}$$

Mathematically, the ISL is computed by the expression

$$ISL = \frac{E}{R_x^2(0)}. \tag{7}$$

Similar to the PSL, the ISL is more conveniently expressed in decibels by the integrated sidelobe level ratio ($ISLR$), using the logarithmic expression

$$ISLR[dB] = 10\log_{10}(ISL). \tag{8}$$

3. Pulse Shaped Phase Coding and Implementation

In a phase-coded pulse modulation, a single pulse is subdivided into N_c number of smaller chips of width τ_c. The phase ϕ_n of each chip is modulated according to the sequences in the code to yield a final modulated sequence given by $x[n] = \exp(-j\phi_n)$, $n = 1, 2, \ldots, N_c$.

The $N_c = 13$ Barker code has only two phases, 0^o and 180^o, that correspond to the amplitude of each chip to be either $+1$ or -1. The Barker-13 code has the sequence of [+1 +1 +1 +1 +1 -1 -1 +1 +1 -1 +1 -1+1].

The polyphase Frank code has a length of N_c, where N_c is a perfect square of some integer ***M***, i.e. $N_c = M^2$. The phase of each chip in the Frank code is computed by the following expression (Richards et. al., 2010)

$$\phi_n = \frac{2\pi}{M} pq \ , \ n = 1,\ldots, N_c \ , \tag{9}$$

where $p, q = 0,\ldots,(M-1)$. There are M different modulo 2π phases in this code.

In the binary codes, the magnitude of the modulated sequences is always unity, while the polyphase Frank codes can have multiple values from 0 to 1. In this work, we have used ***M*** =3 to yield $N_c = 9$ for the Frank code. The different pulse shapes along with their mathematical forms are shown in Table 1. These pulse shapes are applied to individual sub pulse of the respective phase codes. Resulting pulse shape modulated phase code is shown in Fig. 2 for Barker-13 and Fig. 3 for Frank-9.

Table 1: Pulse shapes used and their mathematical forms

PULSE	MATHEMATICAL FORM	SHAPE
Rectangular	$x[n] = 1, (n = 1,..\tau_c)$	
Triangular	$x[n] = 1 - \left\| \frac{n - 0.5\tau_c}{0.5\tau_c} \right\|, (n = 1,..\tau_c)$	
Gaussian	$x[n] = exp\left(-0.5\left(\frac{n - 0.5(\tau_c - 1)}{0.5\sigma(\tau_c - 1)} \right)^2 \right)$	
Exponential	$x[n] = \begin{cases} \exp(\alpha n), n = 1,\ldots,\tau_c \\ \exp(-\alpha n), n = 0.5\tau_c,\ldots\tau_c \end{cases}$	

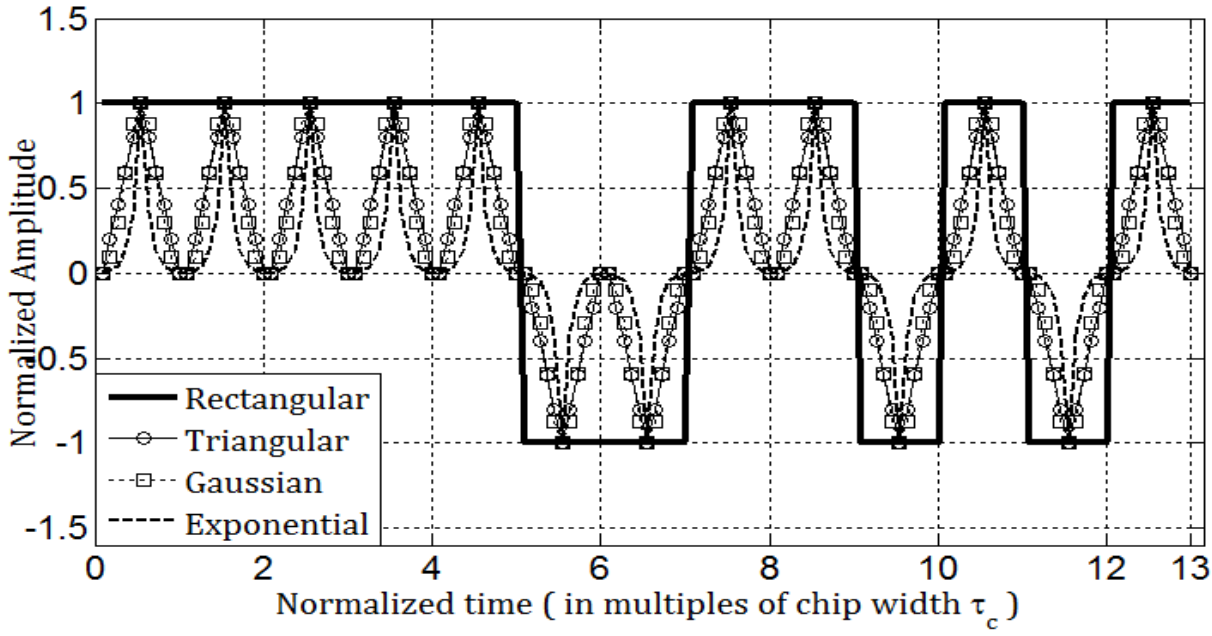

Fig. 2. Barker-13 phase coded pulse for rectangular, triangular, Gaussian, Exponential pulse shapes.

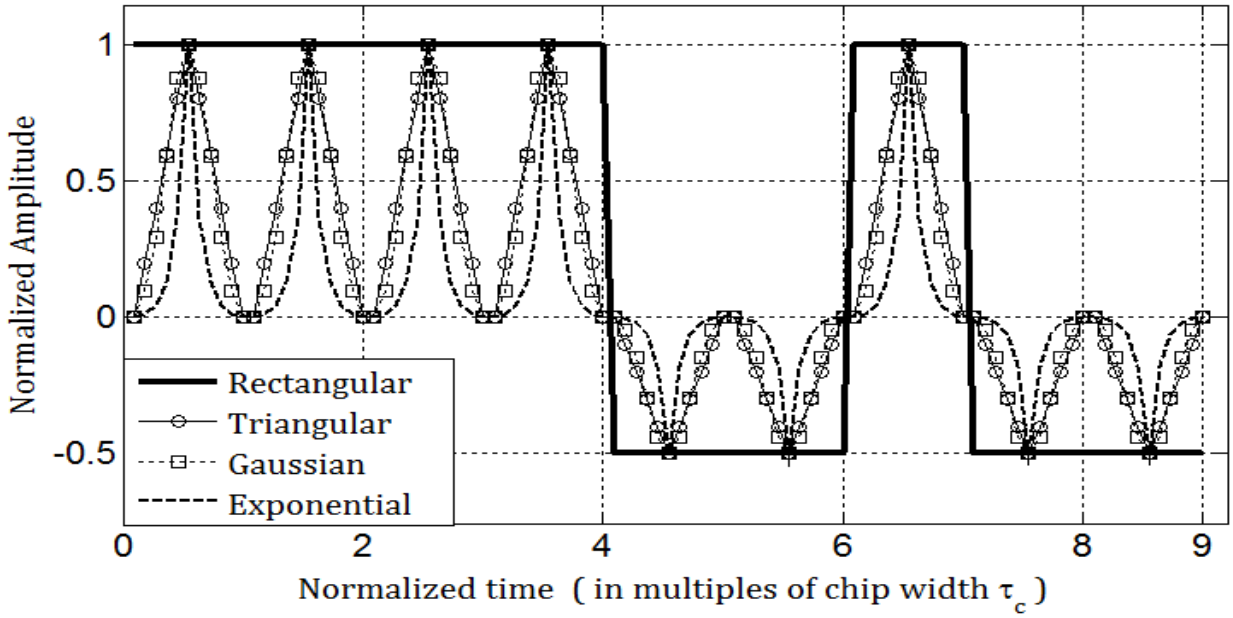

Fig. 3. Frank-9 phase coded pulse for rectangular, triangular, Gaussian, Exponential pulse shapes.

4. Results and Discussions

The normalized autocorrelation function is computed for different pulse shape – phase code combination and is shown in Fig. 4 for Barker-13 and Fig. 5 for frank-9. The performance

parameters of the autocorrelation functions of the Barker and Frank code for different pulse shapes is also computed and summarized in Table 2. In the following sub-sections, we discuss the important observations, related to normalized autocorrelation functions of the Barker and Frank modulated pulse based on Figs. 4 & 5, and Table 2.

4.1 Similarities between autocorrelation functions of Frank-9 and Barker-13 modulated pulses.
With the rectangular pulse as the reference pulse shape, we notice that the non-rectangular pulse shapes have a narrower main lobe width. In both the cases, the ***PSLR*** is $1/N_c$ and as the pulse shape gets narrower from rectangular to exponential, the main lobe of the autocorrelation function also gets narrower. The autocorrelation function of rectangular pulse acts as an envelope to the autocorrelation functions obtained using the non-rectangular pulse shapes.

4.2 Differences between autocorrelation function of Frank-9 and Barker-13 modulated pulses.
While the main lobe and side lobes are clearly separated in the autocorrelation of Barker code for all the pulse shapes, there is a clear separation only with the use of exponential pulse for the autocorrelation of Frank code. Since the Barker code with 13 chips, it yields better sidelobe suppression than the Frank code with 9 chips. In the case of Frank code in Fig. 5 for non-rectangular pulse shapes, we observe that for ***M=3*** phases there are **2** peaks within the envelope of sidelobe obtained from the rectangular pulse. This observation is valid for a larger number of phases ***M***.

4.3 Effect of pulse shaping on the autocorrelation functions
From Fig. 4 and Fig.5, it is clearly seen that the non-rectangular pulse shapes yield a narrower main lobe and sidelobe for both Barker and Frank codes. Among all the four pulse shapes that we have considered, the exponential pulse yields the narrowest mainlobe, narrowest sidelobe, and also it provides a clear distinction from the main lobe and the first sidelobe. Also, the exponential pulse shape yields a higher ***ISLR***.

Table 2 Autocorrelation properties of different code-pulse combinations

PHASE CODE	PULSE SHAPES	RELATIVE 3-dB MAINLOBE WIDTHS	PSLR (dB)	ISLR (dB)
BARKER-13	Rectangular	1.0	-22.278	-8.969
	Triangular	0.7663	-22.278	-7.526
	Gaussian	0.6769	-22.278	-6.977
	Exponential	0.2405	-22.278	-3.484
FRANK-9	Rectangular	1.0	-19.085	-9.539
	Triangular	0.7216	-19.085	-7.851
	Gaussian	0.6375	-19.085	-7.286
	Exponential	0.2265	-19.085	-3.786

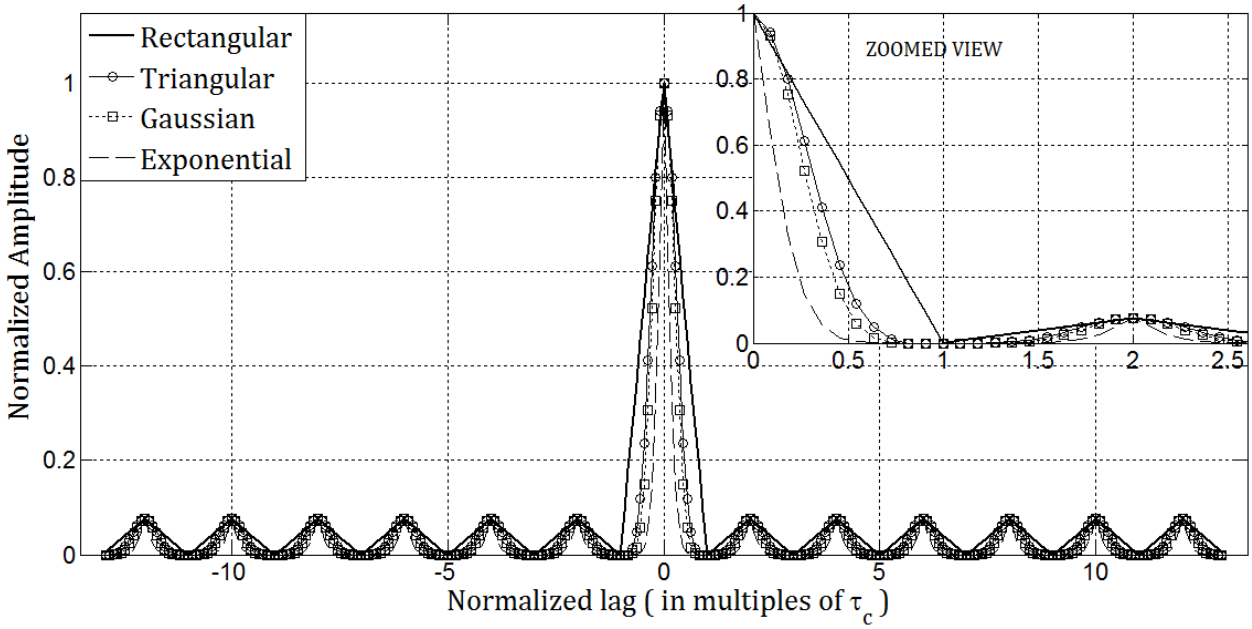

Fig. 4. Normalized autocorrelation function for Barker-13 modulated pulse in Fig. 2.

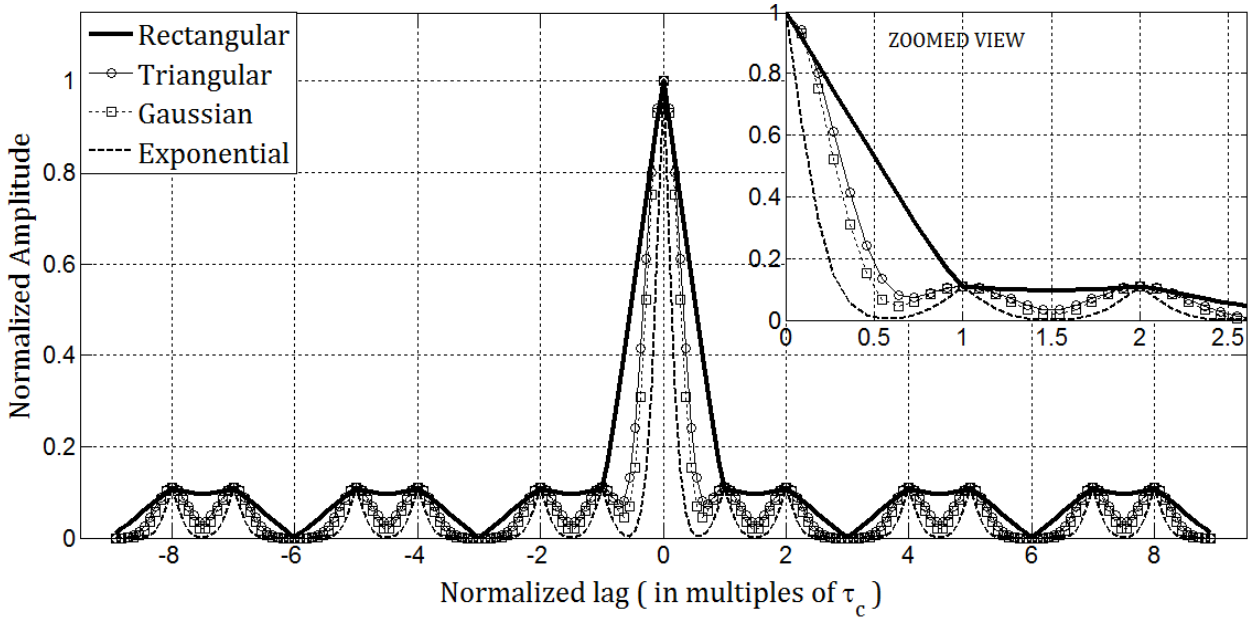

Fig. 5. Normalized autocorrelation function for Frank-9 modulated pulse in Fig. 3.

5. Conclusions

In this paper, we have reviewed the autocorrelation properties that describe the performance of a phase-code modulated pulse. We discussed the commonly used phase codes: binary Barker code

with 13 chips, and polyphase Frank code with 9 chips. The effect of using a narrower pulse shape on the phase coded modulation has been demonstrated. The use of pulse shape affects the 3dB resolution, energy and the ***ISLR,*** but the ***PSLR*** is unaffected by the pulse shape.

5.1 Effect of using different Phase codes

Irrespective of any pulse shape used, the phase-modulated codes used in this work provide a fixed ***PSLR*** of $1/N_c$. The Barker-13 code gives a ***PSLR*** of 1/13 (-22.278 dB), while the Frank-9 code yields 1/9 (-19.085 dB). A phase code with more number of chips provides a better sidelobe suppression performance.

5.2 Effect of using different pulse shapes

In the autocorrelation function of Frank code, by using the rectangular pulse shape, each sidelobe is wide and single domed. But in the case of non-rectangular pulse shapes, multiple peaks are obtained within a sidelobe. The number of peaks is found to be ***M***-1 when ***M*** different phases are used in the Frank code.

Since the energy content of a pulse is dependent on the pulse shape for a given pulse length, the integrated sidelobe ratio depends on the pulse shape. Narrower pulse provides a larger ***ISLR***. The Frank-9 code provides lower ***ISLR*** than the Barker-13 code for a given pulse shape.

For a given phase code and a fixed number of chips, the 3-dB range resolution of the exponential shaped pulse yields the lowest value.

Among the four pulse shapes that we have used in this work, the exponential pulse shape yields the narrowest main lobe, and sharper peaks in sidelobes for both the phase codes. Also in the case of polyphase Frank code, the exponential waveform performed very well in separating the mainlobe and its immediate sidelobe, which was not possible with other pulse shapes that we used. The excellent properties of exponential pulses suggest its potential uses in situations where attenuation of return signal is not prominent. A technique for realization of exponential pulse related to radiation measurements was provided by Jordanov et al. (1994). Some of the possible areas of its applicability include ultrasound imaging, nearby range-finding applications such as collision and obstacle avoidance system in automated robotic machines (Jorg and Berg, 1998), guiding system for visually impaired, eye-safe lidar systems for surveying etc. Exponential signals have potential of realization with the developments in ultrafast circuits. Further investigation on using the double exponential pulse shape in phase codes could reveal much more interesting features in its autocorrelation properties.

References

Barker, R.H., (1953). Group synchronizing of binary digital systems, *Communication Theory* (W. Jackson, ed.), Academic Press, New York, pp. 273–287

Frank, R. L., (1963). Polyphase codes with good nonperiodic correlation properties, *IEEE Transactions on Information Theory*, vol.9, no.1, pp. 43-45. http://dx.doi.org/10.1109/TIT.1963.1057798

Jordanov, V.T., Knoll, G.F., Huber, A.C, Pantazis, J.A., (1994). Digital techniques for real-time pulse shaping in radiation measurements, *Nuclear Instruments and Methods in Physics Research*, A353, pp. 261-264. http://dx.doi.org/10.1016/0168-9002(94)91652-7

Jorg, K. -W. and Berg. M., (1998). Mobile Robot Sonar Sensing with Pseudo Random Codes, *IEEE International Conference on Robotics and Automation*, Belgium, pp. 2807-2812 http://dx.doi.org/10.1109/ROBOT.1998.680476

Li, Y., (2009). 3D Laser Pulse Shaping, Measurement, and 3d Electron Beam Profile Measurement for Photoinjectors, *Proceedings of ERL09*, Ithaca, New York, pp. 40-44.

Nunn, C.J., Coxson, G.E., (2008).Best-known autocorrelation peak sidelobe levels for binary codes of length 71 to 105, *IEEE Transactions on Electronic Systems*, vol.44, no.1, pp. 392-395. http://dx.doi.org/10.1109/TAES.2008.4517015

Richards, M.A., Scheer, J. A., Holm, W.A., (2010). *Principles of Modern Radar*, Raleigh, NC: Scitech Publishing Inc., ISBN-9781891121524

Schafhuber, D., Matz, G., Hlawatsch, F., (2002). Pulse-shaping OFDM/BFDM systems for time-varying channels: ISI/ICI analysis, optimal pulse design, and efficient implementation, *The 13th IEEE International Symposium on Personal, Indoor and Mobile Radio Communications,* Vol.3, no., pp. 1012-1016, vol.3, 15-18, http://dx.doi.org/10.1109/PIMRC.2002.1045180

Weiner, A.M.,(2011). Ultrafast optical pulse shaping: A tutorial review, *Optics Communications*, Volume 284, Issue 15, 15 July, pp. 3669-3692, ISSN 0030-4018. http://dx.doi.org/10.1016/j.optcom.2011.03.084

Yurchak , B.S., (2012). An Exponential Model of Radar Altimeter Waveform, *ESA Conference on Earth Observation and Cryospheric Science*, Frascati, Italy, November 13-16.